

whether anti- or proapoptotic BCL-2 members exert a dominant role. Our studies indicate that in vivo, intact cells require a multidomain proapoptotic member to respond to a diverse set of death signals. tBID must activate BAX or BAK to initiate mitochondrial dysfunction and cell death in hepatocytes and MEFs. Conceivably, in other tissues, this function may be served by other proapoptotic multidomain family members such as BOK (25). Activation and oligomerization of BAX or BAK have been proposed to result in formation of a homomultimeric pore (9, 26), formation of a voltage-dependent anion channel-containing pore (27), or permeabilization of mitochondrial membranes (28) to initiate cytochrome c release. Release of cytochrome c activates the Apaf-1-Caspase-9 apoptosome and downstream effector caspases (13), and after substantial loss of cytochrome c, progressive caspase-independent mitochondrial dysfunction can lead to cell death (29). Knockouts of cytochrome c or Caspase-9 and Apaf-1, which function downstream of mitochondria, indicate that damage from staurosporine, etoposide, and radiation depends on signals mediated by cytochrome c release from mitochondria (17–21). The *Bax*, *Bak*-deficient cells, which have a block immediately upstream of mitochondria, appear even better protected from these agents. Even ER stress-induced apoptosis requires BAX or BAK, which might reflect undefined roles of BAX or BAK at ER sites (30, 31) or an ultimate dependence of ER pathways on mitochondria (32). Other upstream activators of BAX and BAK clearly exist, as *Bid*-deficient cells are often susceptible to stimuli that fail to kill cells lacking both BAX and BAK. Our loss-of-function studies reveal that the absence of proapoptotic BAX and BAK molecules creates a profound block, preserving mitochondria and inhibiting apoptosis after seemingly unrelated signals initiated at multiple sites including plasma membrane, nucleus, and ER.

References and Notes

1. D. R. Green, *Cell* **102**, 1 (2000).
2. G. Kroemer, J. C. Reed, *Nature Med.* **6**, 513 (2000).
3. J. M. Adams, S. Cory, *Science* **281**, 1322 (1998).
4. A. Gross, J. M. McDonnell, S. J. Korsmeyer, *Genes Dev.* **13**, 1899 (1999).
5. D. C. Huang, A. Strasser, *Cell* **103**, 839 (2000).
6. H. Li, H. Zhu, C. J. Xu, J. Yuan, *Cell* **94**, 491 (1998).
7. X. Luo, I. Budihardjo, H. Zou, C. Slaughter, X. Wang, *Cell* **94**, 481 (1998).
8. A. Gross et al., *J. Biol. Chem.* **274**, 1156 (1999).
9. M. C. Wei et al., *Genes Dev.* **14**, 2060 (2000).
10. R. Eskes, S. Desagher, B. Antonsson, J. C. Martinou, *Mol. Cell Biol.* **20**, 929 (2000).
11. L. Van Parijs et al., *Immunity* **11**, 281 (1999).
12. M. C. Wei, W.-X. Zong, unpublished data.
13. P. Li et al., *Cell* **91**, 479 (1997).
14. X. M. Yin et al., *Nature* **400**, 886 (1999).
15. T. Lindsten et al., *Mol. Cell* **6**, 1389 (2000).
16. C. Scaffidi et al., *EMBO J.* **17**, 1675 (1998).
17. R. Hakem et al., *Cell* **94**, 339 (1998).
18. K. Kuida et al., *Cell* **94**, 325 (1998).
19. H. Yoshida et al., *Cell* **94**, 739 (1998).
20. F. Cecconi, G. Alvarez-Bolado, B. I. Meyer, K. A. Roth, P. Gruss, *Cell* **94**, 727 (1998).
21. K. Li et al., *Cell* **101**, 389 (2000).

22. R. J. Kaufman, *Genes Dev.* **13**, 1211 (1999).
23. T. Nakagawa et al., *Nature* **403**, 98 (2000).
24. H. He, M. Lam, T. S. McCormick, C. W. Distelhorst, *J. Cell Biol.* **138**, 1219 (1997).
25. S. Y. Hsu, A. Kaipia, E. McGee, M. Lomeli, A. J. Hsueh, *Proc. Natl. Acad. Sci. U.S.A.* **94**, 12401 (1997).
26. M. Saito, S. J. Korsmeyer, P. H. Schlesinger, *Nature Cell Biol.* **2**, 553 (2000).
27. S. Shimizu, M. Narita, Y. Tsujimoto, *Nature* **399**, 483 (1999).
28. R. M. Kluck et al., *J. Cell Biol.* **147**, 809 (1999).
29. V. K. Mootha et al., *EMBO J.* **20**, 661 (2001).
30. W. Zhu et al., *EMBO J.* **15**, 4130 (1996).
31. F. W. Ng et al., *J. Cell Biol.* **139**, 327 (1997).
32. J. Hacki et al., *Oncogene* **19**, 2286 (2000).
33. D. S. Ory, B. A. Neugeboren, R. C. Mulligan, *Proc. Natl. Acad. Sci. U.S.A.* **93**, 11400 (1996).
34. Primary murine embryonic fibroblasts were generated from *Bax*^{+/-};*Bak*^{+/-} or *Bax*^{+/-};*Bak*^{-/-} timed matings at 13.5 days after conception. Primary MEFs were immortalized by transfection with a plasmid containing SV40 genomic DNA. Primary MEFs were plated in six-well plates and were transfected with 1 μg of total DNA using Fugene (Roche) according to

the manufacturer's instructions. Stable immortalized clones were generated through serial dilution.

35. Cells were fixed in 3% paraformaldehyde and permeabilized in 1% bovine serum albumin and 0.1% Triton X-100. Cells were sequentially incubated with primary antibody to cytochrome c (clone 6H2.B4, Pharmingen) and Cy3-conjugated goat secondary antibody to mouse (Jackson ImmunoResearch Laboratories) and Hoechst 33258 (Molecular Probes) and then mounted under a cover slip with *N*-propyl gallate. Images were acquired with a SPOT camera (Diagnostics) mounted on Nikon Eclipse E600 with PlanFluor objectives or Olympus IX50 microscopes.
36. We thank E. Smith for figure and manuscript preparation, B. Avery and S. Wade for animal husbandry, C. Gramm for technical assistance, C. Beard for assistance with retrovirus, P. Tegtmeyer for SV40 expression vector, and W. Sellers for use of the microinjector. M.C.W. is supported in part by NIH training grant 5T32AT09361. W.-X.Z. is supported by a postdoctoral grant from the Cancer Research Institute. This work is supported in part by NIH grants R01CA50239 and R37CA48023.

17 January 2001; accepted 29 March 2001

Allosteric Control of RNA Polymerase by a Site That Contacts Nascent RNA Hairpins

Innokenti Touloukhonov,*† Irina Artsimovitch,* Robert Landick‡

DNA, RNA, and regulatory molecules control gene expression through interactions with RNA polymerase (RNAP). We show that a short α helix at the tip of the flaplike domain that covers the RNA exit channel of RNAP contacts a nascent RNA stem-loop structure (hairpin) that inhibits transcription, and that this flap-tip helix is required for activity of the regulatory protein NusA. Protein-RNA cross-linking, molecular modeling, and effects of alterations in RNAP and RNA all suggest that a tripartite interaction of RNAP, NusA, and the hairpin inhibits nucleotide addition in the active site, which is located 65 angstroms away. These findings favor an allosteric model for regulation of transcript elongation.

Evolutionarily conserved, multisubunit RNAPs transcribe genes into RNAs in all known organisms. A universal feature of these RNAPs is a regulated conversion from an initiating form that holds the RNA weakly, to an elongating form that holds RNA tightly during RNA synthesis, and then back to a terminating form that releases RNA. The molecular basis of this switch is unknown. However, conservation from bacteria to humans of RNAP's core subunit composition ($\beta'\beta\alpha_2$ in bacteria), amino acid sequences, three-dimensional structure, and contacts to DNA and RNA suggest that the switch will be similar for all multisubunit RNAPs (1–3).

A nascent RNA hairpin can terminate tran-

scription by bacterial RNAP if the hairpin includes the 3 to 5 nucleotides (nt) usually found in the RNA exit channel and disrupts at least 1 base pair (bp) of the \sim 8-bp nascent RNA: template DNA hybrid that is present in stable transcription elongation complexes (TECs) (4–7). Similar RNA hairpins can also pause, rather than terminate, transcription when they form more upstream but near the RNA:DNA hybrid, rather than invade it. Both hairpin-dependent pausing and termination can be enhanced by the universal bacterial protein NusA (8, 9).

Two models can explain hairpin effects on transcription (3, 7, 10–15). In the rigid-body model, a pause or terminator hairpin begins forming when only its loop and upper stem have emerged from the exit channel, and then pulls RNA through the channel and away from the active site to avoid steric clash with a rigid RNAP as the lower stem pairs. This partially unwinds the RNA:DNA hybrid and moves RNAP forward without nucleotide addition [the hybrid is wedged against the upstream edge of the active-site cleft in a TEC; see fig. 4A in

Department of Bacteriology, University of Wisconsin, Madison, WI 53706, USA.

*These authors contributed equally to this work.
 †On leave from the Limnological Institute, Russian Academy of Sciences, Irkutsk, Russia.
 ‡To whom correspondence should be addressed. E-mail: landick@bact.wisc.edu

REPORTS

(3)]. In the allosteric model, once the hairpin starts to form, it instead triggers a conformational change in RNAP that inhibits nucleotide addition in the active site and reduces affinity for product RNA, without necessarily moving the intervening RNA.

To test the rigid-body versus allosteric models, we examined a pause hairpin that inhibits nucleotide addition by a factor of 10 to 20 at the *Escherichia coli his* pause site (16). The pause hairpin loop substituted with 5-iodoU photocrosslinks strongly to RNAP's β -subunit flap domain between residues 903 and 952, causing an unusual retardation of β during SDS-polyacrylamide gel electrophoresis (SDS-PAGE) relative to RNA- β cross-links in nonpaused TECs (17). This cross-link also occurs with a 5-iodoU-substituted tetraloop pause hairpin (Fig. 1), which pauses equivalently to wild-type (8) and whose structure is known (18), or when 4-thioU is used in place of 5-iodoU (19). 5-IodoU, but not 4-thioU, preferentially cross-links to Phe, Tyr, Trp, Met, and His residues (20), which are found between β 903-952 only at F906 and F934 (Fig. 1B). F906 is the likely target of hairpin-loop cross-linking because the strong, shifted- β band disappeared when we used a β F906A, but not a β F934A, mutant RNAP (Fig. 1C) (21). To confirm this, we established that (i) 5-iodoU or 4-thioU in the hairpin loop cross-linked between trypsin cleavage at amino acid position 903 and 2-nitro-5-thiocyanobenzoic acid cleavage at position 909 (in β K909C RNAP) (19) and (ii) 4-thioU cross-linking was retained in the β F906A mutant, showing that F906A does not alter hairpin-flap interaction (19).

F906 is located in a short α helix at the tip of RNAP's flap domain (1). The flap is flexibly connected to RNAP, held open by lattice forces in a crystal structure, and thought to close over the exiting RNA in a TEC (1, 3, 22), probably by contact of a hydrophobic patch on the flap-tip helix to the clamp domain of RNAP (Fig. 2). When we modeled the pause hairpin into a TEC structure (3), using the reported position of the -11 nt (the nt immediately 3' of the hairpin) and the loop contact to the flap-tip helix, the hairpin fit under the open flap domain (Fig. 2B) (19). Thus, unless the RNA exit channel closes in the TEC by either flap or clamp movement, the steric clash predicted by the rigid-body model would not occur. If the exit channel closes as expected, the hairpin could pull the RNA (including the -11 nt) through the channel and away from the active site, while retaining loop contact to the flap-tip helix. Alternatively, the hairpin could open the exit channel, potentially generating an allosteric signal.

To distinguish these possibilities, we tested three predictions of the rigid-body model: (i) hairpin formation should move the -11 nt, (ii) lengthening the 3-nt spacer between the hairpin and hybrid should reduce the hairpin's ability to pull RNA away from the active site and thus to

stimulate pausing, and (iii) stabilizing the hairpin by lengthening its stem should increase its stimulation of pausing.

To map its contacts to RNAP, we substituted the -11 nt with 4-thioU (5-iodoU cross-linked poorly at -11). Separately, we substituted the 3'-terminal nt with 5-iodoU. We performed photocrosslinking in the paused TEC,

or after hybridization of an antisense oligonucleotide that converts it to a rapidly elongating TEC (Fig. 3A) (6, 19). As predicted by both models, 3'-nt contacts changed upon paused TEC formation (β' : β ratio changed, Fig. 3A), but no change was detected in the -11 nt position even when we mapped it to a 6 Å by 9 Å area where the mapped segments of β and β'



Fig. 1. Pause hairpin cross-linking. (A) Structures of wild-type and tetraloop *his* pause RNAs with positions of analog (magenta) or ³²P (*) incorporation, the -11 and +1 nt (green), the spacer RNA present in the exit channel (color-on-black), and the RNA:DNA hybrid (underlined) indicated. (B) Amino acid sequence around the previously identified cross-link target in *E. coli* RNAP (β 903–952) (17). -- Δ --, flap-tip deletion. Likely targets of 5-iodoU cross-linking are shown in red. (C) Cross-linking of the tetraloop pause hairpin to wild-type, β F906A, and β F934A RNAPs. TECs containing 5-iodoU and [³²P]cytidine monophosphate (Fig. 1A) were halted at -9, -3, and the pause as described (17). After irradiation at 308 nm, samples were denatured, subjected to SDS-PAGE, and visualized by phosphorimaging. Abbreviations for the amino acid residues are as follows: A, Ala; D, Asp; E, Glu; F, Phe; G, Gly; I, Ile; K, Lys; L, Leu; M, Met; N, Asn; P, Pro; Q, Gln; R, Arg; S, Ser; T, Thr; and V, Val.

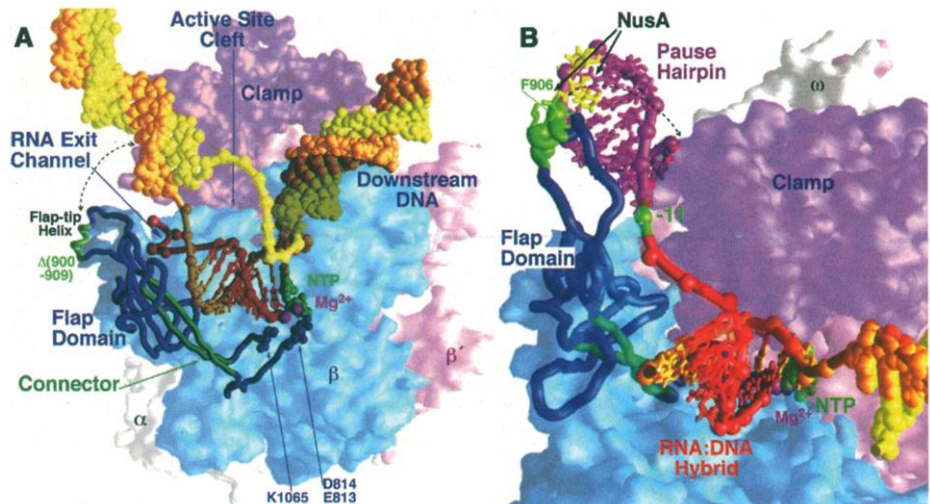


Fig. 2. Model of pause hairpin formation in a TEC. (A) RNAP (α and ω , white; β , light blue; β' , pink) is rendered semitransparent to reveal key internal features and contents of the active-site cleft. The flap (dark blue worm) and clamp (violet) domains form the RNA exit channel. The flap domain connects to K1065 and E813/D814 in the active site (Mg^{2+} , magenta; NTP, green) through the antiparallel β -sheet connector (green). Flap-tip residues deleted in $\beta\Delta(900-909)$ are in green. Template DNA (orange), nontemplate DNA (yellow), and RNA (red) are positioned as in (3). The dotted arrow indicates likely closure of the exit channel. (B) Pause hairpin-RNAP interaction magnified and rotated left 30° and down 60° relative to (A). Upstream DNA removed for clarity. The tetraloop pause RNA hairpin magenta was positioned by the -11 nt (green) and the loop uridines (yellow) that cross-link to F906 (green spacefill). Hydrophobic-patch residues (L901, L902, I905; green) may contact β or β' (dotted line) in a TEC. Possible NusA interactions are indicated by arrows.

cross-linking overlapped (Fig. 3, B and C). This also is the previously reported -11-nt location (3), validating our modeling of the pause hairpin. If hairpin formation were to move -11 more than 1 nt, cross-linking to this small area would not be maintained (nt in single-stranded, extended RNA are separated by ≥ 7.5 Å) (Fig. 3C), and even slight movement likely would

alter the β' : β ratio (see Fig. 3A). To determine the effects of spacer length, we varied it from 2 to 5 nt (Fig. 4A). When the spacer was increased to 4 nt, hairpin-dependent pausing increased, directly contradicting the rigid-body model. Hairpins with 2- or 5-nt spacing supported pausing if NusA was present.

To examine the effects of lengthening the

hairpin stem, we changed it from 5 to 8 bp (using the optimal 4-nt spacer). Hairpin-dependent pausing was lost without NusA, again contradicting the rigid-body model (Fig. 4A). Although hairpin shape and location are important for pausing, all the spacer and stem results are readily explained by specific hairpin interactions with RNAP and NusA.

Together, these results and previous findings make a convincing case against the rigid-body model: (i) the pause hairpin cannot be initiated by antisense oligonucleotide pairing to nascent RNA (6); (ii) unraveling of the RNA:DNA hybrid, required if hairpin formation pulls RNA through the exit channel, does not occur in a paused TEC (23); (iii) the hairpin creates steric clash with RNAP, as required by the rigid-body model, only if the RNA exit channel closes in the TEC (Fig. 2), yet the hairpin fails to move the -11 nt, as it must if the exit channel remains closed (Fig. 3); and (iv) increasing the spacer length increases pausing (Fig. 4A), whereas increasing the hairpin stem-length reduces pausing (24) (Fig. 4), both opposite to the rigid-body model's predictions. We conclude that steric effects of a pause hairpin on RNA translocation through a rigid RNAP alone cannot explain hairpin-dependent pausing. The hairpin must cause some conformational change in RNAP, for which flap or clamp movement is the apparent trigger.

Because NusA enhancement of pausing requires the pause hairpin (8, 15), made suboptimal pause signals work better (Fig. 4A), and is modulated by the structure of the hairpin loop (8) (e.g., compare tetraloop to wild type in Fig. 4A), we wondered if NusA also acts through interaction with the flap-tip helix, either directly or by contacting the hairpin loop. When NusA was added to paused TECs containing 5-iodoU-substituted hairpin loops, strong, retarded-gel mobility cross-linking to β F906 was replaced by weaker cross-linking to NusA (Fig. 4B, lanes 2 and 3). Both the NusA and shifted- β cross-links disappeared when the hairpin was disrupted with an antisense oligonucleotide, and did not occur in nonpaused TECs at -9 (Fig. 4B, lanes 4 to 7).

To determine whether the flap-tip helix was required for pausing and NusA action, we prepared and tested an RNAP lacking the helix [Figs. 1A and 2A, $\beta\Delta(900-909)$ (19, 21). In the absence of NusA, the helix deletion reduced hairpin stimulation of pausing from ~ 10 -fold to ~ 2 -fold (Fig. 4A). The helix deletion completely abolished NusA enhancement of pausing (Fig. 4A) and NusA's ability to slow transcription elsewhere (19). Thus, the flap-tip helix is required for regulation of pausing by NusA and for most of the pause hairpin's effect.

We propose that NusA stabilizes pause hairpin-flap interaction, which, by opening the RNA exit channel, may allosterically affect RNAP's active site. Interaction of the

Fig. 3. The -11 nt does not move upon paused TEC formation. (A) Phosphorimage of β' and β separated by SDS-PAGE after cross-linking in paused and nonpaused (with antisense oligonucleotide) TECs with 4-thioU at -11 or 5-iodoU at the 3' end. (B) Single-hit, partial cyanogen bromide cleavage of β' and β subunits cross-linked by 5-iodoU at -11 in paused and nonpaused TECs (3). Cross-links were assigned between the cleavage site closest to the NH_2 - or COOH -terminus that removed the radioactive label and the adjacent site at which cleavage yielded a radioactive fragment. (C) Location of the -11 nt (green) in paused and nonpaused TECs based on results in (B) (19). Orange, region of β' cross-link. Blue, region of β cross-link. Magenta, the 6 Å by 9 Å area in which the mapped regions of cross-linking to β and β' overlap. The flap is removed (dark green outline) to reveal an extended, single-stranded RNA (red) in the exit channel.

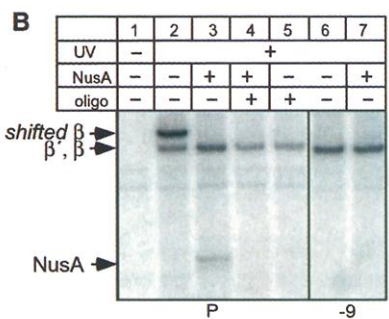
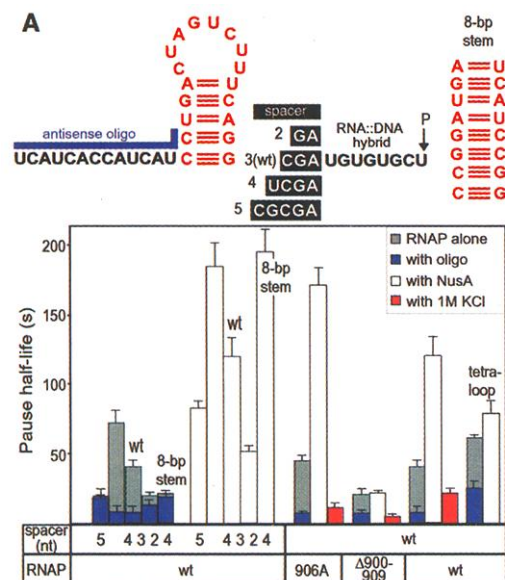
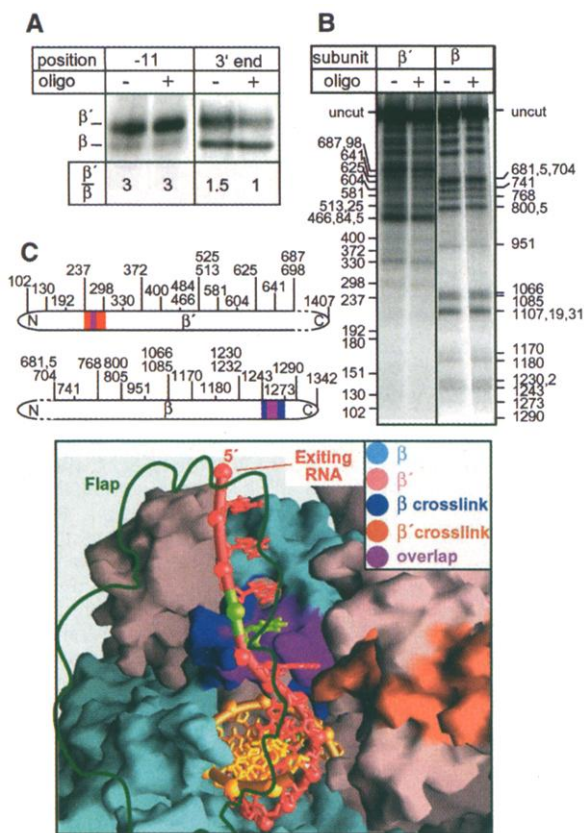


Fig. 4. Effects of hairpin-spacing, stem-length, flap-tip helix, and NusA on pausing. (A) Pause half-lives (gray bars) were measured as described (7, 19). The residual half-life with antisense oligonucleotide (blue) or 1 M KCl (red) reveals the hairpin's contribution to pausing (15). Antisense oligonucleotides for the tetraloop and 8-bp stem pause sites were extended to include pairing to the hairpin loop. (B) TECs with 5-iodoU and ^{32}P in the hairpin

loop (Fig. 1A) were halted at -9 or the pause, combined with antisense oligonucleotide or NusA as indicated, irradiated at 308 nm, subjected to SDS-PAGE, and phosphorimaged.

composite NusA-β-subunit surface with RNA may stabilize RNA structures and explain NusA's ability to accelerate cotranscriptional folding of RNA (25).

How might an allosteric signal generated by flap contact affect catalysis in the active site, which is 65 Å from the flap-tip helix? The flap domain connects to RNAP through a two-stranded, antiparallel β sheet (the connector). The connector runs along the active-site cleft to highly conserved amino acids in the active site (E813, D814, and K1065; Fig. 2). E813 and D814 may chelate the Mg²⁺ ion bound to the substrate nucleoside triphosphate (NTP); K1065 contacts the α phosphate of the 3'-terminal RNA nt; substitution of E813 or K1065 disrupts catalysis (26, 27). Therefore, the pause hairpin may affect catalysis by moving the flap and, by way of the connector, critical residues in RNAP's active site. Alternatively, hairpin formation could open the active-site cleft by moving the clamp domain. Conversely, flap or clamp movement and possibly hairpin formation could be inhibited when NTPs bind efficiently (because bound NTP would constrain the position of E813/D814), and may be coupled to movements of parts of RNAP that form the active-site cleft and downstream DNA jaws (Fig. 2) (13).

Definition of the flap-tip helix as an allosteric site on RNAP provides a new framework for understanding RNAP's regulation. σ also binds RNAP's flap (28); σ may open the RNA exit channel to thread RNA into the channel; σ release may allow the channel to close for efficient transcript elongation (13). Like pause hairpins, terminator hairpins probably also open the RNA exit channel, rather than pull RNA out of RNAP, and then dissociate the TEC by invading the RNA:DNA hybrid, opening the active-site cleft, and triggering collapse of the transcription bubble (3, 6). Finally, eukaryotic RNAPs also contain a flap domain, making the flap an attractive target for both prokaryotic and eukaryotic regulators of transcription.

References and Notes

1. G. Zhang *et al.*, *Cell* **98**, 811 (1999).
2. P. Cramer *et al.*, *Science* **288**, 640 (2000).
3. N. Korzheva *et al.*, *Science* **289**, 619 (2000).
4. E. Nudler, A. Mustaev, E. Lukhtanov, A. Goldfarb, *Cell* **89**, 33 (1997).
5. I. Sidorenkov, N. Komissarova, M. Kashlev, *Mol. Cell* **2**, 55 (1998).
6. I. Artsimovitch, R. Landick, *Genes Dev.* **12**, 3110 (1998).
7. W. S. Yarnell, J. W. Roberts, *Science* **284**, 611 (1999).
8. C. L. Chan, R. Landick, *J. Mol. Biol.* **233**, 25 (1993).
9. C. D. Sigmund, E. A. Morgan, *Biochemistry* **27**, 5622 (1988).
10. P. J. Farnham, T. Platt, *Cell* **20**, 739 (1980).
11. T. D. Yager, P. H. von Hippel, *Biochemistry* **30**, 1097 (1991).
12. I. Gusarov, E. Nudler, *Mol. Cell* **3**, 495 (1999).
13. R. A. Mooney, R. Landick, *Cell* **98**, 687 (1999).
14. R. J. Davenport, G. J. Wuite, R. Landick, C. Bustamante, *Science* **287**, 2497 (2000).
15. I. Artsimovitch, R. Landick, *Proc. Natl. Acad. Sci. U.S.A.* **97**, 7090 (2000).
16. The *his* pause synchronizes transcription with trans-

- lation in the attenuation control region of the *E. coli his* operon (8). The pause signal is multipartite; interactions of downstream DNA, 3'-proximal RNA, and NTP substrate, together with the pause hairpin, inhibit nucleotide addition by a factor of ~100 (8).
17. D. Wang, K. Severinov, R. Landick, *Proc. Natl. Acad. Sci. U.S.A.* **94**, 8433 (1997).
18. E. Ennifar *et al.*, *J. Mol. Biol.* **304**, 35 (2000).
19. Supplementary data are available on Science Online at www.sciencemag.org/cgi/content/full/292/5517/730/DC1.
20. K. Meisenheimer, T. Koch, *Crit. Rev. Biochem. Mol. Biol.* **32**, 101 (1997).
21. RNAP subunits (α, NH₂-terminally His₆-tagged wild-type or mutant β, and β' carrying a COOH-terminal intein and chitin-binding domain) were co-overexpressed in *E. coli*. After sonication and capture of RNAP on a chitin matrix (New England Biolabs), RNAP was recovered by dithiothreitol-mediated intein cleavage. βF934A RNAP paused equivalently to wild-type RNAP; βF906A RNAP pausing was more sensitive to competition by Cl⁻; βΔ(900-909) RNAP pausing was reduced at

- both low and high [Cl⁻] (Fig. 4). TEC synthesis and photocross-linking were performed as described (17).
22. R. D. Finn, E. V. Orlova, B. Gowen, M. Buck, M. van Heel, *EMBO J.* **19**, 6833 (2000).
23. D. N. Lee, R. Landick, *J. Mol. Biol.* **228**, 759 (1992).
24. C. Chan, D. Wang, R. Landick, *J. Mol. Biol.* **268**, 54 (1997).
25. T. Pan, I. Artsimovitch, X. W. Fang, R. Landick, T. R. Sosnick, *Proc. Natl. Acad. Sci. U.S.A.* **96**, 9545 (1999).
26. A. Mustaev *et al.*, *J. Biol. Chem.* **266**, 23927 (1991).
27. V. Sagitov, V. Nikiforov, A. Goldfarb, *J. Biol. Chem.* **268**, 2195 (1993).
28. T. Gruber, I. Artsimovitch, K. Geszvain, R. Landick, C. Gross, unpublished data.
29. We thank S. Darst for help in molecular modeling and pointing out the possible role of βED813/814; K. Murakami for sharing an RNAP overexpression plasmid; M. Barker, R. Gourse, R. Saeccker, M. Sharp, and members of our lab for helpful suggestions; and the NIH for support (GM38660).

27 November 2000; accepted 28 March 2001

Reversible Unfolding of Single RNA Molecules by Mechanical Force

Jan Liphardt,¹ Bibiana Onoa,¹ Steven B. Smith,² Ignacio Tinoco Jr.,¹ Carlos Bustamante^{1,2*}

Here we use mechanical force to induce the unfolding and refolding of single RNA molecules: a simple RNA hairpin, a molecule containing a three-helix junction, and the P5abc domain of the *Tetrahymena thermophila* ribozyme. All three molecules (P5abc only in the absence of Mg²⁺) can be mechanically unfolded at equilibrium, and when kept at constant force within a critical force range, are bi-stable and hop between folded and unfolded states. We determine the force-dependent equilibrium constants for folding/unfolding these single RNA molecules and the positions of their transition states along the reaction coordinate.

RNA molecules must fold into specific three-dimensional shapes to perform catalysis. However, bulk studies of folding are often frustrated by the presence of multiple species and multiple folding pathways, whereas single-molecule studies can follow folding/unfolding trajectories of individual molecules (1). Furthermore, in mechanically induced unfolding, the reaction can be followed along a well-defined coordinate, the molecular end-to-end distance (*x*).

We studied three types of RNA molecules representing major structural units of large RNA assemblies. P5ab (Fig. 1A) is a simple RNA hairpin that typifies the basic unit of RNA structure, an A-form double helix. P5abcΔA has an additional helix and thus a three-helix junction. Finally, P5abc is comparatively complex and contains an A-rich bulge, enabling

P5abc to pack into a stable tertiary structure (a metal-ion core) in the presence of Mg²⁺ ions (2–9).

The individual RNA molecules were attached to polystyrene beads by RNA/DNA hybrid “handles” (Fig. 1B) (10). One bead was held in a force-measuring optical trap, and the other bead was linked to a piezo-electric actuator through a micropipette (11, 12). When the handles alone were pulled, the force increased monotonically with extension (Fig. 2A, red line), but when the handles with the P5ab RNA were pulled, the force-extension curve was interrupted at 14.5 pN by an ~18-nm plateau (black curve), consistent with complete unfolding of the hairpin. The force of 14.5 pN is similar to that required to unzip DNA helices (13, 14). P5ab switched from the folded to the unfolded state, and vice-versa, in less than 10 ms and without intermediates. Forward and reverse curves nearly coincided, indicating thermal equilibrium. The variation of folding/unfolding force (SD 0.4 pN) reflects the stochastic nature of a thermally facilitated process. Indeed, a plot of the fraction unfolded versus force (Fig. 2B, dots) is fit well by the statistics of a two-

¹Department of Chemistry and ²Departments of Physics and Molecular and Cell Biology, Howard Hughes Medical Institute, University of California, Berkeley, CA 94720, USA.

*To whom correspondence should be addressed. E-mail: carlos@alice.berkeley.edu